SMART BED AND CONTACT IMPACT OF FLEXIBLE BODIES USING ENERGY COMPENSATION METHOD

by

PRANAV PARIKH

Presented to the Faculty of the Graduate School of
The University of Texas at Arlington in Partial Fulfillment
of the Requirements
for the Degree of

MASTER OF SCIENCE IN MECHANICAL ENGINEERING

THE UNIVERSITY OF TEXAS AT ARLINGTON

December 2015

ॐ

भूर्भुवः स्वः

तत्सवितुर्वरिण्यं

भर्गो देवस्य धीमहि

धियो यो नः प्रचोदयात् ॥

To my parents, Bharat and Nayana Parikh, and my beloved sisters Rachana and Vyoma Parikh, whose guidance and support have made me who I am today.

ACKNOWLEDGEMENTS

I would like to thank my supervising professor Dr. Alan Bowling for constantly motivating and encouraging me, and also for his invaluable advice during the course of my graduate study. I wish to thank Dr. K. Lawrence and Dr. B. P. Wang for their interest in my research and for taking time to serve in my thesis committee.

I would like to thank all my current and past friends and colleagues from The Robotics, Biomechanics and Dynamic Systems Lab. Dr. Mahdi Haghshenas-Jaryani for their patient guidance and support during my initial days in the lab. Abhishekh Chaterjee, Ashley Chase Guy, Nachiket Kansara,Rohit Katti,and Yatish Nagraj for all their support and valuable feedback regarding my work and also for being good companions in the lab.

I would like to express my deepest gratitude to my mother, Nayana Parikh, late father Bharat Parikh, my sisters Vyoma and Rachana Parikh, without whose support and sacrifices, it would have been impossible for me to continue working hard. I would also like to thank my brother in law Rupesh Shah, my sweet Nephew Kreteyu Shah for encouraging me time to time. I would like to remember my late grand parents Mahendra, and Kala Parikh, and my maternal grand parents Dileep and late Pragnya Munim. Also thanking my cousin sisters Bindiya Desai, Ami Patel, Kripa Patel, Puja Mehta, Anisha Gupta, Prosobee Sanghvi, Smita Shah, Ushma Mehta and Vidhi Shah. A very special thanks to Kalia family (Dharamvir and Urmila Kalia, along with their 4 daughters, Sweety, Preeti, Niti, and Kirti), who have loved me since I was born, I will always remember you all. Also thanking my friend Kshitija Suryawanshi for supporting me all the time.

Special thanks to Piyush and Jyotsna Shah, and Mahendra and Neeta Thakar, for helping me and my family in all the ways they could.

I proudly dedicate my work to my Mother, Father and Sisters.

November 20, 2015

ABSTRACT

SMART BED AND CONTACT IMPACT OF FLEXIBLE BODIES
USING ENERGY COMPENSATION METHOD

Pranav Parikh, M.S.

The University of Texas at Arlington, 2015

Supervising Professor: Alan P. Bowling

This work investigates robotic means to prevent pressure ulcers in human bodies. The smart bed is intended to act as an intelligent assistant to a caregiver that relieves some of the physical and mental burden involved in preventing pressure ulcers. This type of device is needed because of a labor shortage in the nursing field. The smart bed distinguishes itself from the current available measures by redistributing pressure and minimizing shear forces acting on the skin in contact. This is done by using data from the sensor grid installed on the bed surface and actuating the degrees of freedom associated with the smart bed.

Interaction with human body needs contact and impact analysis. Using computational dynamics and computer simulations, a human body is approximated with a flexible object. By doing impact analysis using energy compensation method, and checking the energy consistency we can study the interaction, and validate the correctness of the results.

TABLE OF CONTENTS

LIST OF ILLUSTRATIONS

CHAPTER 1

INTRODUCTION

1.1 Pressure Ulcers:

Pressure ulcer is commonly termed as bed-sore, decubitus ulcer or pressure sore and sometimes as pressure necrosis or ischemic ulcer. The term pressure ulcer was popularized by the Agency for Health care Research and Quality. Pressure ulcer has been defined as an area of unrelieved pressure usually over a bony prominence leading to ischemia, cell death and tissue necrosis. This definition has been further refined by the National Pressure Ulcer Advisory Panel (NPUAP) and European Pressure Ulcer Advisory Panel (EPUAP) as localized injury to the skin and/or underlying tissue usually over a bony prominence as a result of pressure, or pressure in combination with shear and/or friction [http://www.npuap.org/].

Pressure ulcers are a cause of concern since a very long time. Its mention and effective treatment procedures are very well known and discussed amongst ancient Indian, and Egyptian civilizations. Triphala, a compound formulation of the herb

Figure 1.1. Stage 4.

Figure 1.2. Early and Late Stage.

Terminalia Chebula, Phyllanthus Emblica, and Terminalia Bellerica has been described in the Ayurveda (ancient Indian system of medicine) as a tridoshic rasayan, having balancing and rejuvenating effects on the 3 constitutional elements that govern human life [2]. Triphala is 1 of the important antioxidant rich rasayana drugs that has been reported to treat chronic ulcers. Another important natural antiseptic is Honey, which is a fast and cheap home remedy [3].

In the present time, pressure ulcers are still a great deal of concern. Many studies have been done to know the prevalence of pressure ulcers in hospital patients. Data from the National Nursing Home Survey, 2004 says, about 159,000 current U.S. nursing home residents (11%) had pressure ulcers [4]. From about 2% to 28% of nursing home residents have pressure ulcers. A major factor contributing in treatment of pressure ulcers is Nurses, dissatisfaction among them can create a great deal of problem. With that motivation Smart Bed is developed with an aim to reduce the role of care givers. Looking at the seriousness of the situation November 19th was celebrated as World Wide Pressure Ulcer Prevention Day [$http : //www.npuap.org/$].

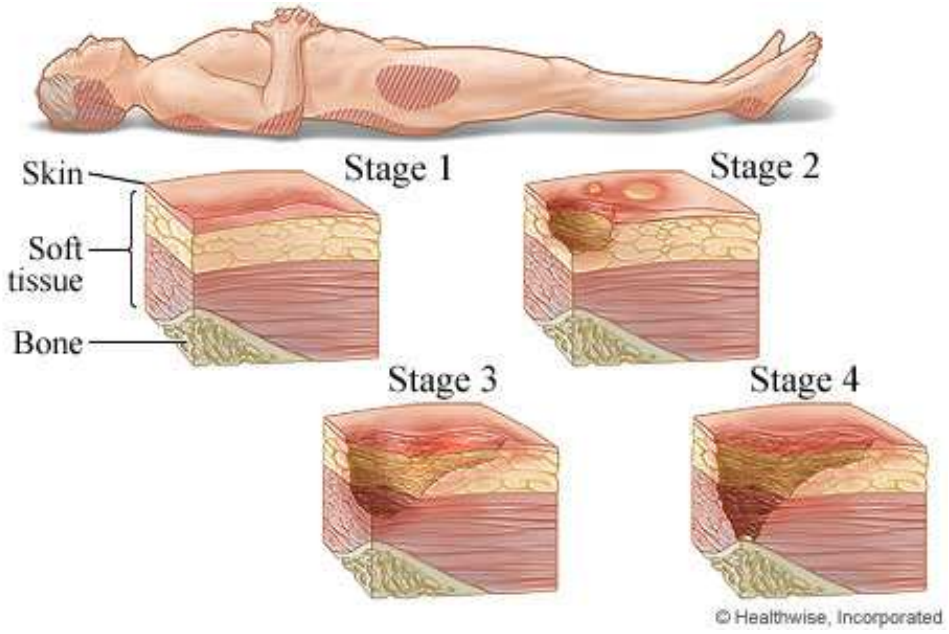

Figure 1.3. 4 Stage Symptoms.

Fig 1.3 [*http* : *//img.webmd.com/dtmcms/live/webmd/consumer_assets/site_images/media/medical/hw/h*9991533_002.*jpg*]. The most common system for staging pressure ulcers classifies them based on the depth of soft tissue damage, ranging from the least severe (stage 1) to the most severe (stage 4). There is persistent redness of skin in stage 1; a loss of partial thickness of skin appearing as an abrasion, blister, or shallow crater in stage 2; a loss of full thickness of skin, presented as a deep crater in stage 3; and a loss of full thickness of skin exposing muscle or bone in stage 4.Of the 1.5 million current U.S. nursing home residents in 2004, about 159,000 (11%) had pressure ulcers of any stage. Stage 2 was the most common (5%), accounting for about 50% of all pressure ulcers. Stages 1, 3, and 4 made up about the other 50% of all ulcers [4].

Pressure Ulcers occur in many situations, most vulnerable patients are nursing home admits, people with trauma cases,and people with physical disabilities [5]. 17% to 35% of patients have pressure ulcers at the time of admission to a nursing home,

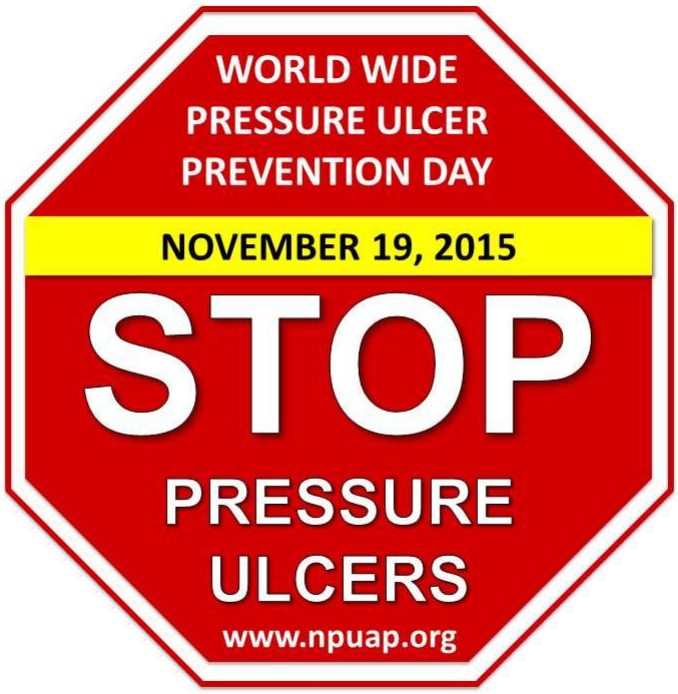

Figure 1.4. World Wide Pressure Ulcer Prevention Day.

and the prevalence of pressure ulcers among nursing home residents ranges from 7% to 23%. Among high-risk patients, the incidence of pressure ulcers is estimated to be 14/1000 patient-days. Residents at higher risk for developing ulcers are those who have limited ability to reposition themselves, can-not sense the need to reposition, have fecal incontinence, or cannot feed themselves [5].

Fig 1.4 [$http://www.npuap.org/$]. One could use temporary preventive measures like water bed, and massage bed, but they are helpful in certain cases only, and are not that efficient to a larger extent. Thus a permanent solution is much needed which minimizes if not eliminate the role of care takers in treating pressure ulcer patients.

1.2 Rigid Body Model:

Smart bed is made up of 28 tiles, each tile would be capable of having 3-dof. These 3 degrees of freedom would be imparted by using individual motors to each screw of the 3 screws of the tile. The screws are connected to the motors by a worm gear. A special mechanism connects the screw to the top square plate which is further discussed in chapter 2.

1.3 Flexible Body Model:

Each of the 28 tiles of smart bed will be attached with individually operated and controlled air inflated flexible bladder. This flexible bladder houses more than 730 pressure and shear sensors [6] [7] [8]. The sensors are connected to the control system of the bed which directs the motion according to the sensed pressure and shear forces. The bladder is made of a flexible material such as PVC, and the sensors are designed such that it blends with the bladder material. Detailed description of the flexible model of the smart bed is provided in chapter 3. This work doesn't give more emphasis on sensor design and usage, it is assumed that the sensors can sense pH, pressure, and shear.

1.4 Contact and Impact analysis:

The smart bed would eventually be tested with human body. In order to test the bed with the human body it first needs to be tested with an equivalent system, such as a flexible object like a ball or a cylinder. In this work impact of flexible bodies like a vertical spring, a box, a truss structure, a cylinder, and a ball is analyzed using energy compensation method. In this method the kinetic energy lost

by the point in contact is compensated with the point in immediate vicinity. Energy consistency is tested for all the test objects, and they turn out to be consistent.

CHAPTER 2

SMART BED MODEL DESIGN: RIGID BODY MODEL

2.1 General Idea

The smart bed model can be divided into the Rigid Body model and Flexible Body model. The rigid model comprises of the tile unit, and the flexible model comprises of the inflatable bladder which is attached to the top of the tile. The Smart Bed is an assembly of 28 such tiles, each tile has 3 degrees of freedom, which is driven by worm and screw assembly. The assembly is actuated by 3 motors which moves the screws up and down, through the worm gears, as a result the tile moves. A bladder is attached to the top of the tile base which has an array of sensors. The network of sensors senses shear and pressure forces.

The use of smart bed is focused on redistributing the pressure, so that the favorable condition for developing the pressure ulcer doesn't occur (periodic, cyclic loading is desirable if not necessary for the total prevention of PUs [9] [10]). The redistribution of pressure is done by moving the patient without the help of caregiver or a nurse. The movement in this case is not that much so as it throws the patient out of the bed, but is sufficient enough to distribute the pressure. The control system in the smart bed is designed to be capable of judging the amount of movement that needs to be made. The sensor grid on the surface acts as an transducer to convert the pressure and shear into control signals. Though the smart bed does most of the work, it is advisable that it being operated in constant supervision of a nurse. The process of pressure redistribution can be done illustrated by Fig 2.1 [11].

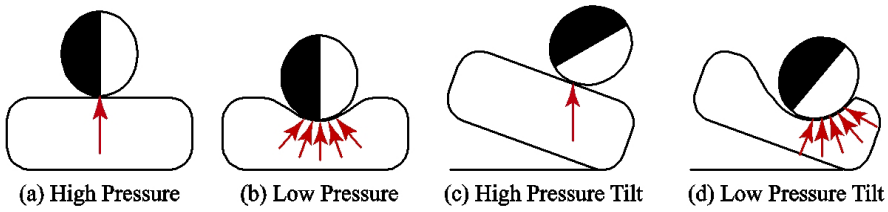

Figure 2.1. Soft Manipulation on Flexible Bladder.

Here the human body is approximated by a flexible object like a ball. In Fig. 2.1(a) , the mattress is very stiff i.e. the internal pressure in the bladder is very high. The object's weight is supported at a single point experiencing a large force, represented by an upward arrow. If the bladder is deflated, the surface sinks, as there is not much pressure to keep the bladder stiff, allowing distribution and reduction of the force at each contact point, as in Fig. 2.1-b. However, the skin is able to stretch, which can increase shear stress, as it sinks into the mattress. In addition, the contact point in Fig. 2.1(a) still experiences a normal force, and may not recover sufficiently. Fig 2.1(c) shows repositioning using a stiff surface. The body rotates and the high force point moves across its surface. However, the force is still large and the body might move from the desired position, as occurs in manually turning the patient. Fig. 2.1(d) shows the smaller, redistributed forces resulting from simultaneous repositioning and deflating the mattress. The original contact point in Fig. 2.1(a) experiences no force, so the skin can recover. Movement of the body during rotation can reduce stretch and shear stress in the skin. The body is likely to remain in the final position and not rotate as far from its original position as in Fig. 2.1(c). Overall, the body has not moved far from its original position, even though the mattress is tilted significantly. Periodically shifting the forces from one side to the other allows the skin on each side to recover, thereby achieving the effect of turning using small rotations.

The rigid body model comprising of the tile assembly will have 3-DOF, which is operated by 3 individual motors. The bladder is flexible and is operated by air pressure, the air pressure allows it to have almost infinite DOF. The combined use of air pressure change and the tilt mechanism forms a unique effect and better controllability than each if used alone.

2.2 Tile Design

The smart bed is made up of 28 units, each unit is called a tile. Tile is as shown in the Fig. 2.2. The tile model is constructed in solid works, and is tested by making a similar structure in Autolev/C++. As in the Fig 2.2, there are 3 worm and gears which are connected to the vertical screws. The screws are motor operated via the worm-gear arrangement. The actuation of the screw depends upon the speed of the motor, and motor to gear ratio. Also the amount of movement of the screw depends upon the motor speed and motor to worm gear ratio. The control signals to the motor would be given by the Micro Controller unit, our focus here will not be into designing the control system, rather we would focus on the dynamic and design study of the structure.

The 3 vertical screws are then connected to a special triangle mechanism via a rotational-prismatic joint. The 3 screws and the rotational-prismatic joints are arranged so that they are spaced at an angle of 120^o with each other. Let the 3 screw be named as A, B, and C. The 3 rotational-prismatic joints be named as D, E,and F. Finally the triangular base be named as G. All the connectors D, E, and F are designed such that they can slide on the respective rod of G on which they are mounted. The rotational joint helps the triangular base to tilt, which intern moves the body on the bladder. Each of the screws are independently connected to the

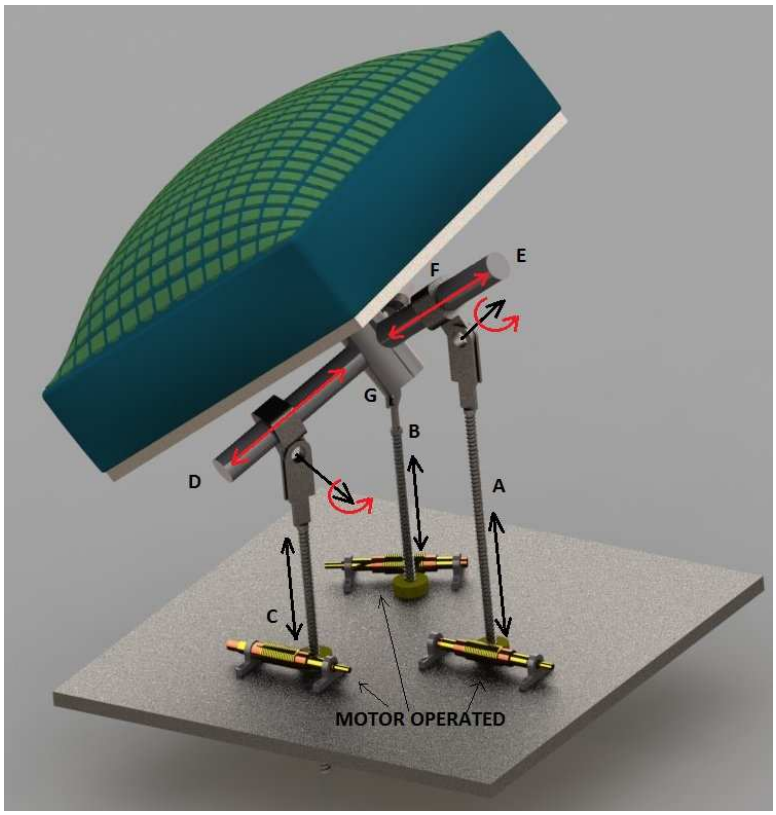

Figure 2.2. Tile Design.

motors, this gives them unique flexibility to move the tile. The triangular base is attached to the tile by a fixed joint.

The kinematics of the the tile is as shown in the Fig 2.3. Let there be a Newtonian point 'N', such that it is fixed to the universal reference frame N. N1 and N2 direction vectors are along the plane of the screen and N3 is in the direction coming out of the screen. A1, B1, C1 are parallel to N1, but is rotated w.r.t the universal reference frame N by a fixed angle. $R_{NA} = 30^o$ and $R_{NB} = 60^o$, $R_{NC} = 0^o$. Let D, E, and F be the joints connecting with A, B, and C, the frames D, E, and F have rotation w.r.t A, B, and C respectively as shown in the Fig 2.3. The frame attached with the tile is G. The tile itself has 2 DOF, which ables it to tilt. The rotations of the frame G is shown in the Fig 2.3. It is to be remembered that a

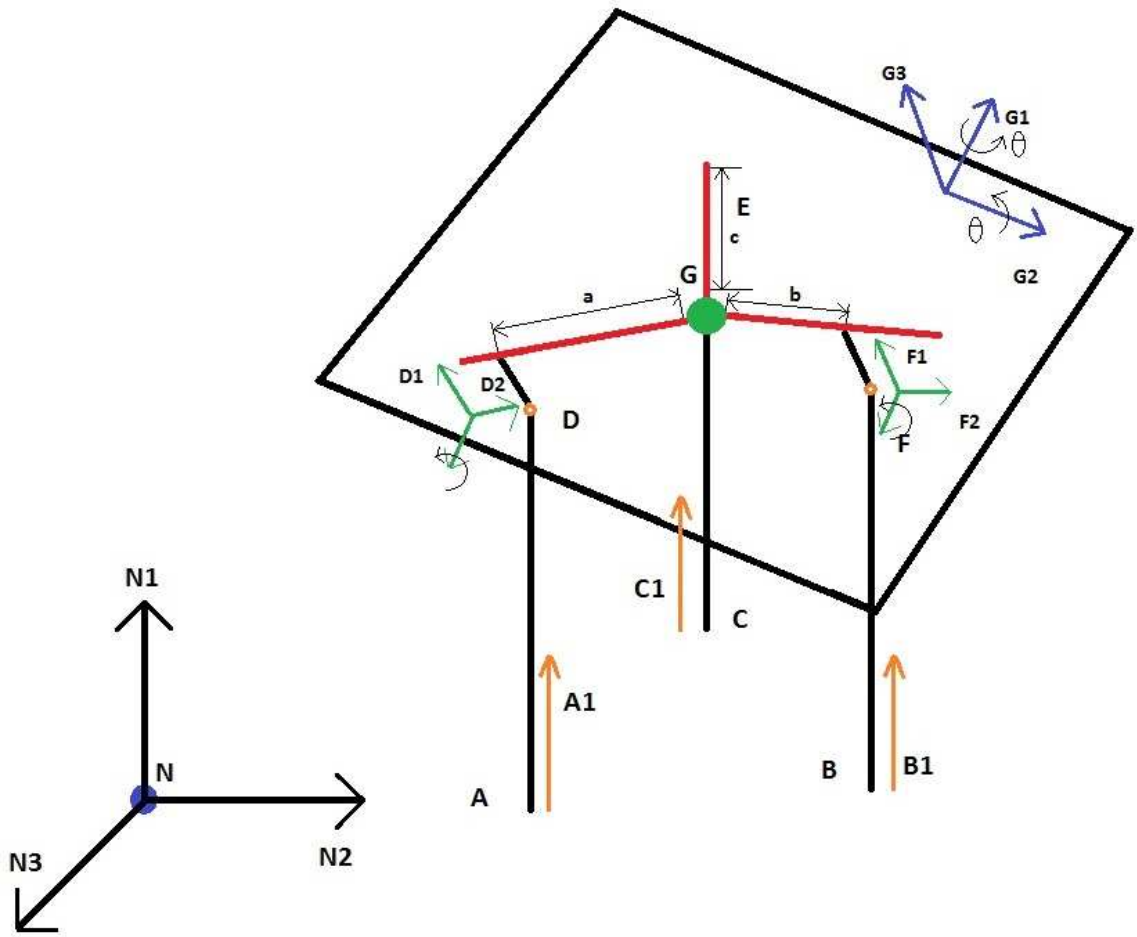

Figure 2.3. Tile Frame Assigment.

frame is never attached to a point, rather it is attached to a body. The orientation of the frame at any point on the body will be same. Also as a result of the rotation of the bodies D, E, and F it slides along the rod connecting the point G, through a prismatic joint. The distance between the connector D and the point G, keeps on changing w.r.t the amount of the angle rotated.

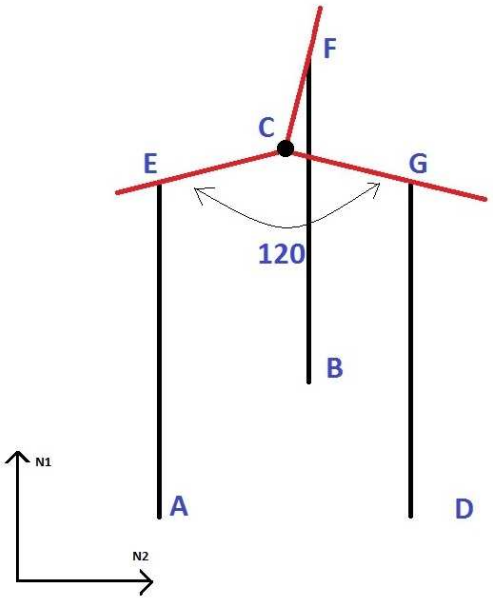

Figure 2.4. Constrained System.

2.3 Constrained System

The tile requires at least 12 generalized coordinates to completely define the system kinematically. The degree of freedom of the system is 3, that means it requires to constrain the other 9 unconstrained variables. Using non holonomic constrain i.e. the loop constrain and the angle constrain we can eliminate those generalized variables.

Fig 2.4. shows the wire frame diagram of the tile, thus by using loop constraint we have:

$$\frac{d}{dt}(P_{AE} + P_{EC} + P_{CG} + P_{GD}) = 0 \tag{2.1}$$

$$\frac{d}{dt}(P_{DG} + P_{GC} + P_{CF} + P_{FB}) = 0 \tag{2.2}$$

P_{AE}=Position vector connecting points A and E.

P_{EC}=Position vector connecting points E and C.

P_{CG}=Position vector connecting points C and G.

P_{GD}=Position vector connecting points G and D.

P_{DG}=Position vector connecting points D and G.

P_{GC}=Position vector connecting points G and C.

P_{CF}=Position vector connecting points C and F.

P_{FB}=Position vector connecting points F and B.

The non-holonomic constraint will eliminate 6 generalized variables, in order to eliminate the rest 3 variables we have to use the angle constraint as shown below:

$$\angle(E-C-G) = \angle(G-C-F) = \angle(F-C-E) = 120^o \tag{2.3}$$

$\angle(E-C-G)$=Angle between points E, C, and G.

$\angle(G-C-F)$=Angle between points G, C, and F.

$\angle(F-C-E)$=Angle between points F, C, and E.

Generalized equation of motion is given by:

$$A\ddot{q} + b(q,\dot{q}) + g(q) = J_c^T F \tag{2.4}$$

q=Generalized Coordinates.

$\dot{q}$=Generalized Velocities.

$\ddot{q}$=Generalized Acceleration.

F=Constrained Forces

Separating $\ddot{q}$ from the equation 2.4 we have:

$$\ddot{q} = \frac{J_c^T F - b(q,\dot{q}) - g(q)}{A} \tag{2.5}$$

Figure 2.5. Bed Tilt.

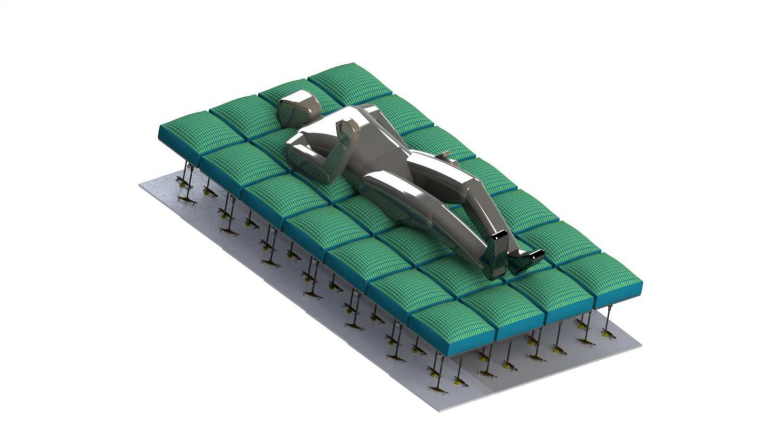

Figure 2.6. Bed with Human.

Equation 2.5 can be integrated numerically to obtain velocities and position values, which could be latter used for simulation. Different methods of integration can be used few of many are Euler's method, Runge-Kutta 4 (RK4),and RK45. Here we have used adaptive RK-45 integrator which is great combination of speed with accuracy.

2.4 Bed Design

The Smart Bed is made of 28 tiles each placed in such a way that there are 7 rows and 4 columns. Each tile is individually operated, depending on the signals obtained from the sensors.

CHAPTER 3

SMART BED MODEL DESIGN: FLEXIBLE BODY MODEL

3.1 General Idea

Flexible body model of the smart bed comprises of the flexible bladder. One of the most difficult task in designing the smart bed is to simulate the flexible body. One of the ways of simulating the flexible system is to discretize the body into various nodes, and connect nodes by spring mass damper. By using bodies we add up extra variables in the system which comes up in defining the body frames. These extra coordinates need to be constrained, using non holonomic constraint, such as loop constraint. Using loop constraint for a simple small planar system is fairly easy. Our aim is to simulate a 3 dimensional mesh made up of more than 730 nodes. Applying loop constraint on such a large system would be very difficult and the simulation time will increase drastically.

Another method of constructing a flexible structure is by considering the nodes to be the point masses. The point masses are then constrained to each other by spring and damper forces. Using spring mass dampers eliminates extra unconstrained variables without using any constraint logic. The calculation required for designing a spring mass damper system is very simple and simulation time reduces very drastically. Different programming tools could be used to simulate such a system, such as C++, Python, Mathematica, or Matlab. By far C++ turns out to be the easiest and fastest one.

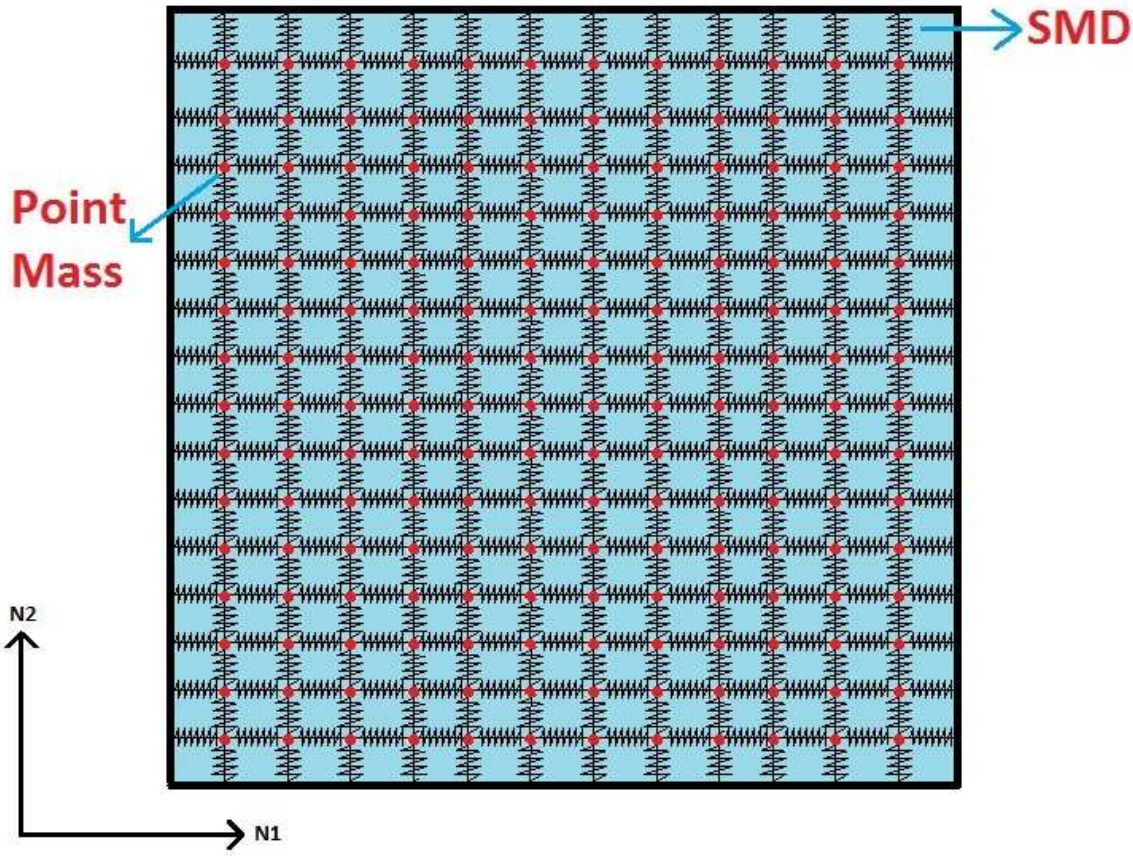

Figure 3.1. Discretized Plate.

As shown in the Fig 3.1 let the square plate be discretized into many nodes, each node represents a point mass shown by a red dot. These red dots are connected with each other by spring force, shown by a black line.

3.2 Spring Mass Damper

Fig 3.2. shows a simple spring damper system with 1 joint connecting two springs. One end of the spring is fixed and other is free to move. As in the Fig 3.2, J is the joint connecting two springs, K is the spring constant, C is the damper

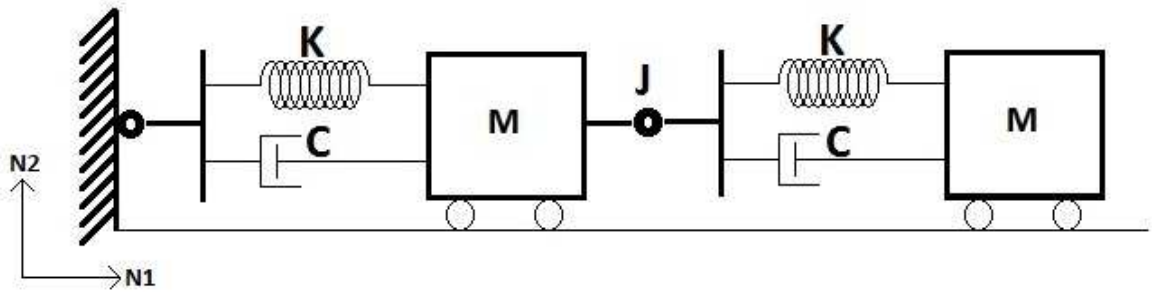

Figure 3.2. Spring Mass Damper.

force, and M is the mass.

Spring Force F_K is given by:

$$F_K = -(K\triangle x)\hat{N}1 \tag{3.1}$$

Damping F_D is given by:

$$F_D{=}F_{Dk}{+}F_{Vd} \tag{3.2}$$

F_D=Internal Spring Damping + Viscous Air Damping

$$\mathbf{a}{=}M^{-1}\ (F_D - F_K) \tag{3.3}$$

"By integrating above equation we can get velocities and position"

3.3 Spring loaded Pendulum

Consider a very simple example of a spring loaded pendulum as shown in Fig 3.3. In the case of a rigid body, the rigid link would experience only gravitational force. The distance between the fixed joint and the end of the link will not change. On the other hand in the case of flexible body the distance between the fixed joint and the end of the link will change. The point mass at the end of the link will

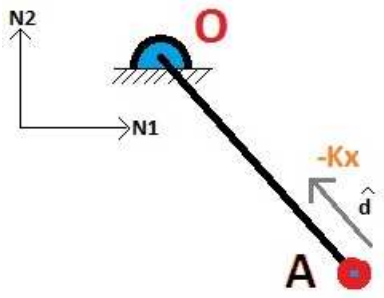

Figure 3.3. Spring Loaded Pendulum.

experience spring force and the damper force.

x=current length of the link.

$\triangle x$= change in the length of the link w.r.t equilibrium

$\triangle x$=1-x (Let the equilibrium length be 1)

The spring force in the flexible link can be given by:

$$F_K = -(K \triangle x)\hat{d} \tag{3.4}$$

K=Spring Constant. where $\hat{d}$ is the direction vector.

$$\hat{d} = \frac{P_{OA}}{magnitude(P_{OA})} \tag{3.5}$$

In the case were the damping value is zero or a very small value, there will be very large deformations in the link. This might tend to failure of integration block. In the physical sense the damping values are very high.

3.4 Planar Closed Loop Flexible Body

Fig 3.4 shows a planar flexible body with 3 links. Here each point mass will try to pull or push the adjacent links into equilibrium position. If no gravity is acting on the system and the point masses are placed such that the link are in equilibrium

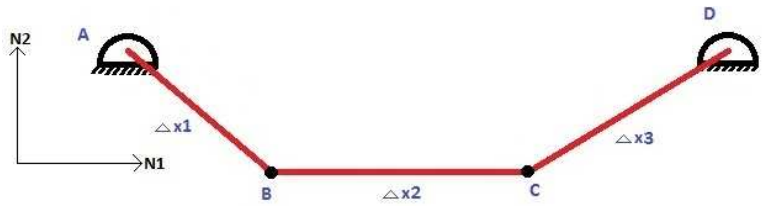

Figure 3.4. Closed Loop Flexible Body.

position then there will be no deformation in the system. With including gravity in the system, it forces the system to change the position. As damping is acting after a finite time the system would come to rest.

Let,

$\triangle x1$= change in the length of the link 1

$\triangle x2$= change in the length of the link 2

$\triangle x3$= change in the length of the link 3

$$F_{AK} = 0 \tag{3.6}$$

$$F_{BK} = (K\triangle x1)d\hat{A} - (K\triangle x2)d\hat{B} \tag{3.7}$$

$$F_{CK} = (K\triangle x2)d\hat{B} - (K\triangle x3)d\hat{C} \tag{3.8}$$

F_{AK}=Spring force at point A.

F_{BK}=Spring force at point B.

F_{CK}=Spring force at point C.

3.5 3 Dimensional Spring Constrained Point Mass

As in the Fig 3.5 a spring constrained point mass, constrained on 4 sides of a square. Here the only forces acting on the point mass are the spring force, the damping force and the gravitational force. Gravitational force is in the -ve N3> direction. Under the effect of gravitation the point mass will tend to move in the -

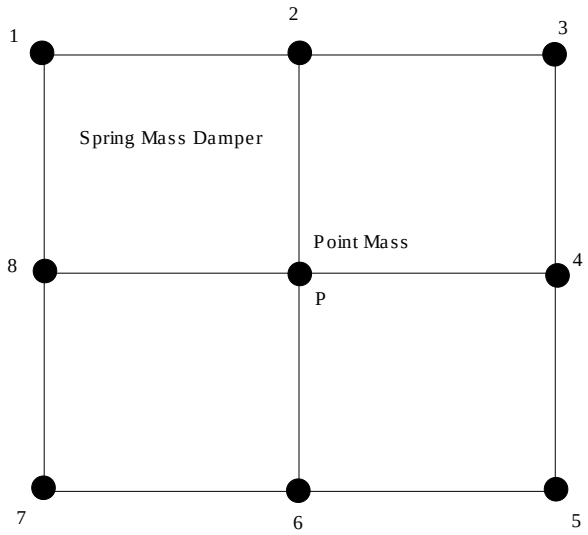

Figure 3.5. Point mass constrained by 4 springs.

N3> direction. As the point mass moves in the - N3> direction, the spring force will act on it, as the spring deforms from its original equilibrium position. The spring force will try to pull the point mass to its original position. The point mass will keep on moving down unless the spring force exceeds or is equal to the gravitational force. The point mass will move up and down as a result of varying spring force. The damping force will keep on reducing the intensity of the vibrations, and after some time the vibrations will turn to zero.

3.6 Generating a Mesh

Generating a mesh is very simple if certain organized steps are followed. Using the method as described to construct a planar flexible body, as in Fig 3.4, as per the amount of point masses a long chain is to be constructed. Here for the flexible bladder we have 730 point masses, the point masses are to divided equally. Starting with the bottom section as in Fig 3.1, first connect all the point masses horizontally. Each chain will have 27 point masses, and there are 27 chains. In order to complete

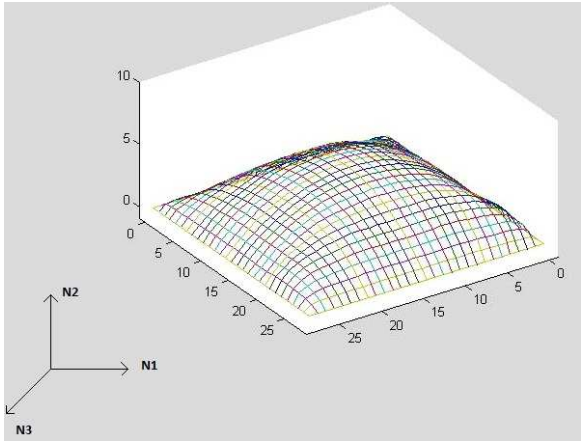

Figure 3.6. Pressurized Mesh.

the mesh each adjacent chain needs to be connected. So we have 28 Spring Mass Dampers-SMD per chain horizontally and vertically.

The logic behind the construction of the mesh is similar to construction of the cloth structure as in [12].

Using Newton's 2^{nd} Law of motion, i.e. F=ma, we have:

$$\begin{bmatrix} F1 \\ F2 \\ F3 \end{bmatrix} = M \begin{bmatrix} a1 \\ a2 \\ a3 \end{bmatrix}$$

Thus,

$$\begin{bmatrix} a1 \\ a2 \\ a3 \end{bmatrix} = M^{-1} \begin{bmatrix} F1 \\ F2 \\ F3 \end{bmatrix}$$

F=Forces on the point masses.

a=acceleration of the point mass.

m=mass.

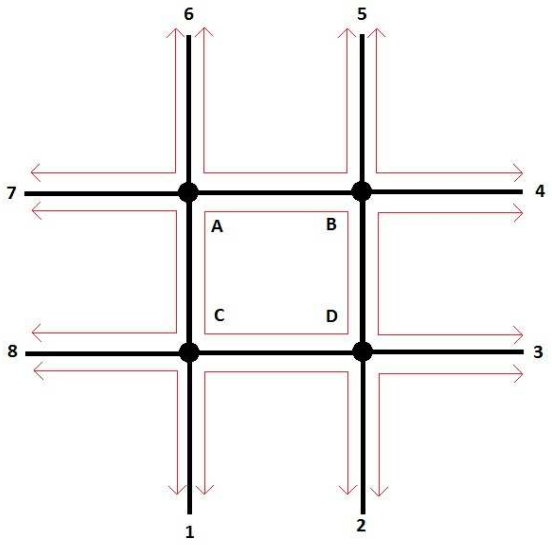

Figure 3.7. Pressure in mesh.

$$\int \mathbf{a} = M^{-1} \int \mathbf{F} \tag{3.9}$$

By integrating the above equation of acceleration we get velocity and position. We can use the velocities and position to simulate a system.

3.7 Pressure Design

Our main aim is to construct a flexible mesh that is air inflatable. Consider the example as shown in Fig 3.5. It shows a small part of the mesh which has 4 point masses in order to apply pressure to this small section we have to take a cross product of the position vector of the springs that connect the point masses. Let, P_C=Pressure at point C, then we have by [13],

$$P_C = P(Cross_{C1-C8} + Cross_{C8-CA} + Cross + CA - CD + Cross_{CD-C1}) \tag{3.10}$$

where,

P=scalar value of pressure.

$Cross_{C1-C8} = Crossproductofpositionvectors P_{C1} and P_{C8}$

$Cross_{C8-CA} = Crossproductofpositionvectors P_{C8} and P_{CA}$

$Cross_{CA-CD} = Crossproductofpositionvectors P_{CA} and P_{CD}$

$Cross_{CD-C1} = Crossproductofpositionvectors P_{CD} and P_{C1}$

The cross products will generate a vector that is perpendicular to the plane formed by the other two vectors. By adding all these perpendicular vectors we will get a resultant vector, which is the resultant pressure directional vector. By multiplying it with a scalar value of pressure P, we get the effect of pressure on the mesh.

There are general misconceptions about point masses behaving in random way when subjected to pressure. If all the values and forces are formated properly the behavior would be proper.

3.8 Assembling Bed and Mesh

Rigid body dynamics is done in Autolev which generates a symbolic code in C++ or Matlab. The simulation time of the code generated from autolev is very long as the code is symbolic. Autolev gives high flexibility for small systems, and the programming is very easy. The method used is based on kane's method for finding equation of motion. Symbolic method is preferable for small systems. For larger systems recursive methods are preferable, like featherstone's algorithm. In the case of system made up of point masses we need not use any of the methods.

3.9 Sensor Design

The work here is concentrated more on the dynamics and design, rather than the instrumentation part. It is assumed that the sensors that we have chosen will work to its standards. An introductory idea of the sensors and its basic design is presented as below.

Each tile in the smart bed includes a parallel mechanism for which some accurate measurement of the joint displacements must be determined. Encoders can be used to determine the displacements for the three legs of tile. It is also possible that additional sensors, such as LVDTs and switches, will be used to provide a home configuration and allow an easier determination of configuration variables in the tile model. Sensors to measure the internal pressures of each air bladder are also included.

3.10 Air Bladder's Sensor Suite

The sensors embedded in the surface of the air bladder are intended to measure the factors that contribute to PU formation in order to facilitate the study of early detection. There are five key issues involved in designing the air bladders surface:

1) sensor configuration,
2) sensor manufacture,
3) sensor number and density,
4) surface manufacture,
5) patient comfort.

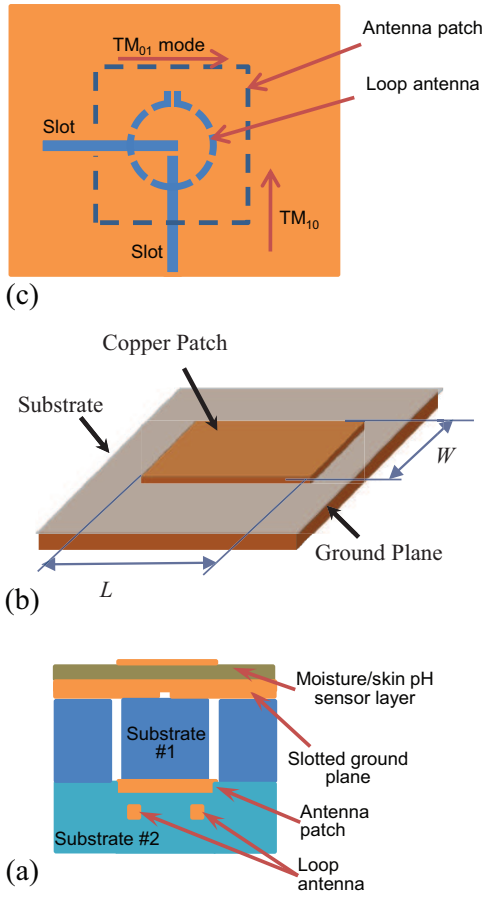

Figure 3.8. Configuration of Sensor Platform.

The sensor network cannot be implemented using commercial off-the-shelf sensors. As such, new types of sensors will be invented for simultaneous pressure, shear, skin pH, and moisture measurement. It is an open problem as to how to accurately measure shear forces in the skin, although preliminary work in this area is promising.

Moisture and Skin pH Sensing Moisture and skin pH can be measured using a micro strip patch antenna [14] [15]. A patch antenna consists of three components: a ground plane, a dielectric substrate, and an radiation patch, see Fig. 3.8(b). Functioning as an electromagnetic resonator, the patch antenna radiates at

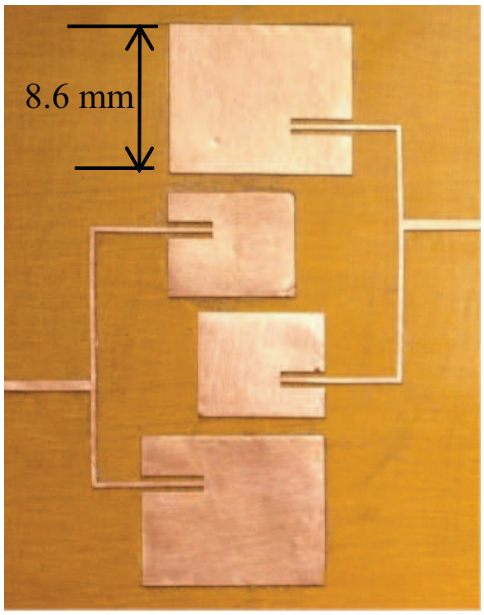

Figure 3.9. Sensor Array.

resonant frequencies that are determined by the dimensions of the radiation patch as well as its effective dielectric constant. The effective dielectric constant, in turn, is determined by the dielectric constant of the medium above the radiation patch and that of the substrate. Moisture and skin pH changes the dielectric constant of human tissue, a change that is measurable from the antenna frequency, if the antenna is placed close to the body.

Shear Sensing Shear forces will be measured using a patch antenna with a slotted ground plane [6]. When a slot is introduced in the ground plane, the current flow in the radiation patch is partially cut off, forcing the current to flow around the slot. As a result, the electric length of the current increases, which reduces the antenna frequency [16]. The configuration of a bi-directional, antenna sensor that can measure shear forces is shown in Fig. 3.8 (c). The antennas f 10 frequency, corresponding to the TM 10 radiation mode, is dependent on the overlapping length between the vertical slot and the antenna patch [16] [17]. Similarly, the f 01 fre-

quency is influenced by the overlapping length between the antenna patch and the horizontal slot. Therefore, the shift of the slots in either direction will cause a shift of the f 01 or f 10 frequencies allowing measurement of shear force. The slots on the ground plane are not through-slots, so the shear sensors are electrically isolated from the moisture/skin pH sensors.

Pressure Sensing A loop antenna will be placed underneath the antenna patch which now serves as a reflector, see Fig. 3.8 (a) [7] [8]. Applying pressure changes the distance between the loop antenna and the reflector, and thus the loop antennas resonant frequency. The patch and loop antennas will be designed to have different resonant frequencies so that there is no coupling between the two antennas. The sensor size is projected to be 5 mm square and 1 cm in height. A unique advantage of the antenna sensors is that they can be multiplexed to form a densely distributed sensor network. Fig. 3.9 shows a four-antenna sensor array that provides a spatial resolution of 1 mm [18].

CHAPTER 4

IMPACT ANALYSIS USING ENERGY COMPENSATION METHOD

4.1 General Idea

As discussed before, the smart bed is to be interacted with human body. In order to study the interaction of human body and the bed i.e. the flexible bladder, we have to study the contact and impact analysis. Different methods of impact analysis are available and are under study. Our focus here is on impact analysis of flexible bodies. Also the first step in studying the impact analysis of flexible bodies, we have to first study its impact with a flat surface. The interaction between flexible bodies is much more difficult than between a flexible body and a hard surface.

The study of flexible body impact can be compared to rigid body impact and are to some extend similar. In the case of rigid body, the relative distance between the point on the body remains constant, while in the case of flexible body the distance between points keep on changing. Understanding the concept given by [19], in which work energy relation is used. Impact force is found at work consumed during impact, the energy lost depends on the coefficient of restitution. If the coefficient of restitution is 1, then the energy lost will be zero. The time taken for rigid body impact is nearly zero, i.e. the rigid body impact is instantaneous. On the other hand the time taken for the flexible body impact takes a non zero time. Impact force could be found by using the newtons 2nd law of motion, this force stops the body from penetrating into the ground. That means the velocity of the point in contact should be zero, but this tends to make the kinetic energy inconsistent. On the other hand if there is no damping in the system there should not be any energy

loss. The Energy Compensation Method, takes care of this and the energy lost is converted into velocity of other particles.

Questions might arise that which points, or how many points should be considered for energy compensation, a detailed description is provided later in the chapter. Different shapes and structures are studies in this work, like a planer spring, double spring, cylinder, truss, prism, and ball. In order to check the analysis I have used energy consistency approach, if the model is right and there is no damping the energy of the system should be consistent or constant.

4.2 Flexible Body Impact

The flexible body analysis is somewhat similar to the rigid body analysis as given by [19]. Let us understand the concept by taking an example of impact of a flexible link or a vertical spring. The flexible spring is constructed by using two point masses, these point masses are force constrained using a spring mass damper equation given by Equ 3.1 and 3.2. By using the newtons second law of motion, i.e. given in equation 3.3 we can simulate the spring. It is always advisable to check the energy without damping before moving to the impact analysis. Using point masses though is very simple and comfortable to use for large systems, it can be tricky if there are errors in programming. The most easy way is to divide the program into different functions like a function for spring mass damper, or making a function for basic shapes like a polygon, or a cube.

Once a system is constructed correctly and energy consistency is checked we can go ahead with the impact analysis. Let us understand it with an example of impact of a vertical spring, be as in the figure 4.1. The values of the spring constant here is taken random and is just for experimental purpose (Spring constant K=5000). The value of damping if applicable is (C=10), and there is no ambient damping in

this case. Using newtons 2nd law of motion and integrating the acceleration we can get the values of velocities and position. The use of velocities and position is very important for this study.

The first step in the impact analysis would be understanding contact, which is discussed in next chapter.

4.3 Contact

Concept of contact will be similar in the case of rigid and flexible bodies. Consider an example of a rigid ball as in the fig 4.3, the forces acting on the rigid ball is gravity. Let the initial position be such that the ball is just touching the ground. In order to stop the ball from going past the ground surface, there should be an equivalent force to stop the ball from penetrating. The force here would be as follows:

$$F_R = F_{Internal} + F_{Gravity} \tag{4.1}$$

The gravitational force here is equal to -9.81$\frac{m}{sec^2}$, and internal force for rigid bodies is 0, while that for the flexible bodies is non zero. It is very important to understand that the contact or equilibrium force is a continuous force unlike that of the Impulse. Its equal in magnitude and opposite in direction to the force exerted by the object on the resting surface.

4.4 Collision

Collision occurs when two objects come in contact with each other, excreting some force. The force in this case is the impact force. Collision is an Instantaneous process, which takes place at infinitesimal time. In order to track the collision an

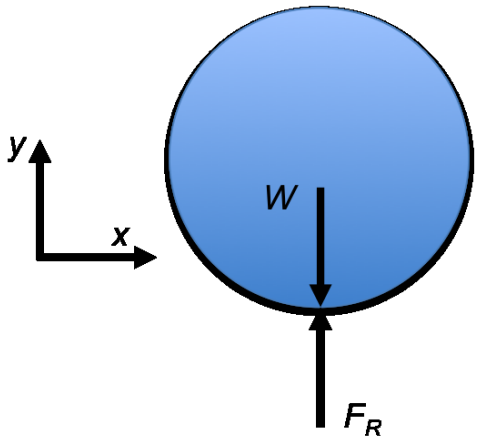

Figure 4.1. Contact.

event function is necessary. The event function is created in C++, which tracks the collision in the integration block.

4.5 Rigid Body Impact

Before going forward with the flexible body analysis, let us first discuss rigid body analysis as given by [19] and [1]. Net work during an impact is given by,

$$W_{1-2} \;=\; T_2 - T_1 \;=\; \frac{1}{2}\,\dot{\mathbf{q}}^T(t+\epsilon)M\;\dot{\mathbf{q}}(t+\epsilon) - \frac{1}{2}\,\dot{\mathbf{q}}^T(t)M\;\dot{\mathbf{q}}(t) \tag{4.2}$$

Normal Work:

$$W_n = \int \mathbf{F}^T d\mathbf{x} = \int \vartheta^T \mathbf{G} dp_{nr} \tag{4.3}$$

The coefficient of restitution (COR) is a measure of the "bounciness" of a collision between two objects: how much of the kinetic energy remains for the objects to rebound from one another vs. how much is lost as heat, or work done deforming the objects.

Stronge's Coefficient of Restitution,

$$W_{nf} \;=\; (1 - e_*^2)W_{nc}[20] \tag{4.4}$$

The impact in rigid bodies can be understood by the work energy plot in Fig 4.1. The Impact process can be divided into 4 phase:

1) Pre-Collision.

2) Collision.

3) Compression.

4) Restitution.

If there is no damping in the system the work done by the system would be constant, i.e. no energy is lost before impact. When the rigid object touches the ground collision is detected, which initiates the impact process. During Impact the first phase is compression, in which the object deforms until the change in work is zero. The work impulse plot plays an important role in study of compression phase. The compression phase is started when the work tends to go -ve i.e. work is done by the system, when the work is minimum, or change in work is zero the compression phase is ended. The amount of energy lost depends on the coefficient of restitution, which is given by Equation 4.3. If the coefficient of restitution in 1, then the work energy plot would end at 0.

4.6 Continuing with Flexible Body Impact

Fig 4.3 shows an example of spring that undergoes impact. The figure shows 5 stages of the impact process:

1)Pre-Impact

2)Impact

3)Reaction

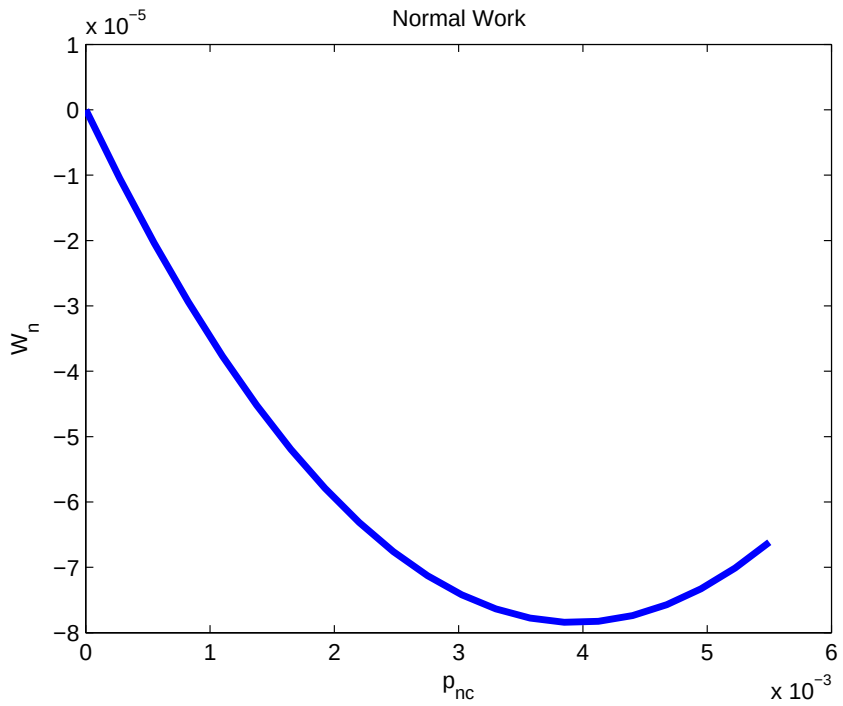

Figure 4.2. Rigid Body Work Plot [1].

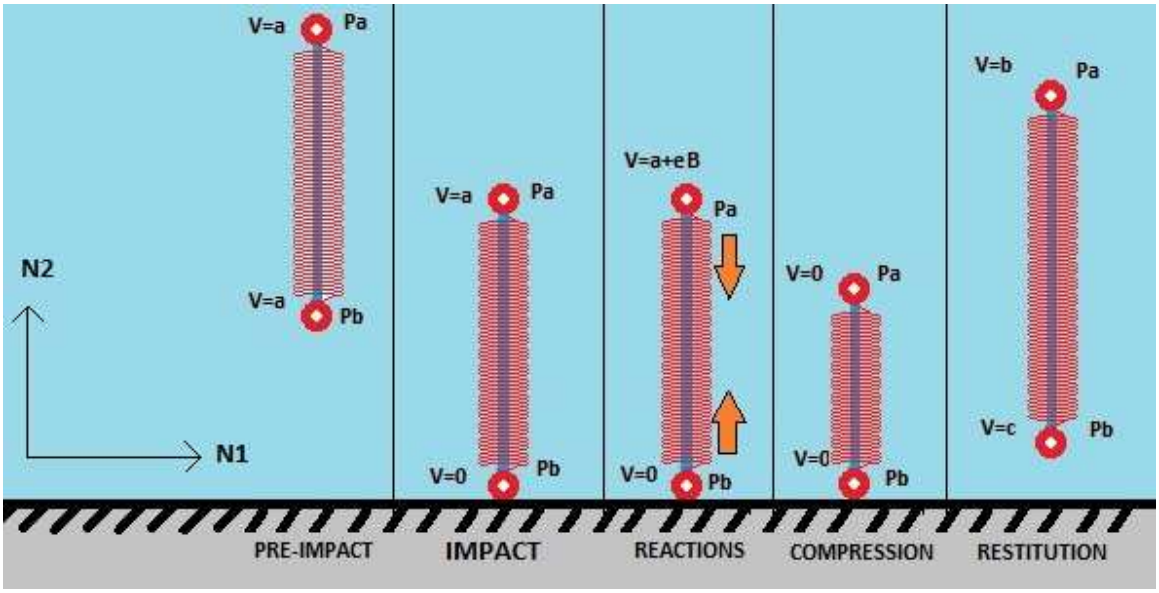

Figure 4.3. Impact Phenomenon.

4)Compression

5)Restitution

Before the impact i.e. when the spring is just released from a height, the spring is under gravitational force. The gravitational force pushes the spring downwards, as a result of some velocity that is induced into it. It is assumed that the spring is not compressed when released from a height. As as result there is no vibration in the spring and it behaves like a rigid body (No internal energy, or potential energy of the spring). When the point B of the spring comes in contact with the ground, i.e. when the vertical component of the position of point B is zero collision occurs or the impact process is initiated. At that moment the points A, and B of the spring will have some velocity let it be 'a'. As a result of the impact the point in contact i.e. point B will undergo instantaneous contraception of its velocity. As the velocity of that point in contact becomes zero there is inconsistency in the energy (assuming there is no damping in the system). The energy calculation is as done below:

$$\textbf{Work=KE + PE}. \tag{4.5}$$

Where,

Work= Normal Work during the impact process.

KE= Total Kinetic Energy of the System

PE= Total Potential Energy of the System

Also we know that,

$$\textbf{KE=}\frac{1}{2}Mv^2 \tag{4.6}$$

v=Velocity of a particle in consideration

M=Mass of the particle, which in our case is equal to 1 as it is a unit mass.

$$\mathbf{PE=PEG + PES} \tag{4.7}$$

PEG=Potential Energy due to gravity

PES=Potential Energy of the Spring Potential Energy due to gravity is given by

$$\mathbf{PEG=Mgh} \tag{4.8}$$

M=Mass of the unity point mass=1.

g=gravitational acceleration.

h=height of the particle from the surface.

$$\mathbf{PES=}\frac{1}{2}K\triangle x^2 \tag{4.9}$$

K=Spring Constant

$\triangle x$= change in the length of the spring with respect to the equilibrium length.

If the energy is calculated at that point it is found that there will be a discontinuity in the energy. This inconsistency in the energy is because of the velocity drop at that instance due to impact. In order to maintain the energy constant we have to make some changes in the velocity of other particles.

$$KE_{BeforeImpact} = \frac{1}{2}[V_{Pa}^2 + V_{Pb}^2] \tag{4.10}$$

$$KE_{Lost} = \frac{1}{2}[V_{Pb}^2] \tag{4.11}$$

$$V_{PaNew}^2 = [V_{Pa}^2 + V_{Pb}^2] \tag{4.12}$$

$$V_{PaNew} = \sqrt{([V_{Pa}^2 + V_{Pb}^2])} \tag{4.13}$$

The kinetic energy before impact can be given by eq 4.10. During the start of the impact the kinetic energy lost will be given by eq 4.11., thus the remaining KE will be due to velocity of point Pa. In order to find the new velocity we have to compensate the energy lost into velocity of the other particle. This is done by equating the energy before impact to the energy of the particle which is not in contact with the ground. Thus the new velocity is found by equation 4.12. This equation is further simplified by eq 4.13 which is the rms value of the velocities before impact. The energy plot during the whole process is as below:

4.7 Work Impulse Relationship

We know that Impulse P can be given by:

$$P = M\triangle v \tag{4.14}$$

Here,

M=mass which is a scalar.

P=Impulse.

$\triangle v$=change in velocity.

v=velocity after the impact.

v_0=velocity before impact.

F=force at the point mass.

W=work done by the point mass.

dx=change in displacement of the point mass.

$$P = M(v - v_0) \tag{4.15}$$

$$\frac{P}{M} = v - v_0 \tag{4.16}$$

$$v = v_0 + \frac{P}{M} \tag{4.17}$$

We also know that Impulse is given by:

$$P = \int F dt \tag{4.18}$$

$$dP = F dt \tag{4.19}$$

$$F = \frac{dP}{dt} \tag{4.20}$$

We also know that Work is given by:

$$W = \int F dx \tag{4.21}$$

$$W = \int \frac{dP}{dt} dx \tag{4.22}$$

$$W = \int dP v \tag{4.23}$$

$$dW = v dP \tag{4.24}$$

from equ 4.17 we can replace v so we get:

$$dW = (v_0 + \frac{P}{M}) dP [21] \tag{4.25}$$

Work impulse plot is constructed by using the equation above, given by [21]. Compression phase ends when the change in work is zero. But at the time of impact the velocity of the point is zero, i.e. $v_0 = 0$. Thus impulse is given by

$$P = Mv \tag{4.26}$$

CHAPTER 5

SIMULATION RESULTS: IMPACT OF DIFFERENT OBJECTS

5.1 Result Analysis

Smart bed is eventually to be tested with human, but interaction with humans require contact and impact analysis. Using the contact and impact simulation technique described in the previous chapter we can simulate the whole process. Impact analysis between flexible bodies is fairly difficult. On the other hand by studying impact analysis between a flexible body and a hard surface and later replicate the method between flexible bodies.

This method is validated with the fact that if there is no damping in the system then there is no energy loss. By plotting the total energy graphs along with Kinetic energy, potential energy, spring potential, and gravity potential we can study the whole process. As shown in the graph the blue line denotes total energy, orange is total kinetic energy, green is total potential energy, purple is gravity potential, and red is spring potential.

By analyzing the graphs shown below we can say that when there is no damping the total energy which is described by the blue line, remains constant. On the other hand due to impact a portion of gravity potential is converted into spring potential or vibrations of the spring. For the case when there is some damping in the system, the total energy would consistently decrease. The system can be validated by the fact that the total energy would always decrease and there is no energy generated by the system. Both the conditions are completely satisfied.

5.2 Test Cases

The method is exemplified by simulating different test cases, such as a spring, double spring, cylinder, truss, prism, and a cube. All the results and plotted and tested using energy consistency method.

The test cases are as below:

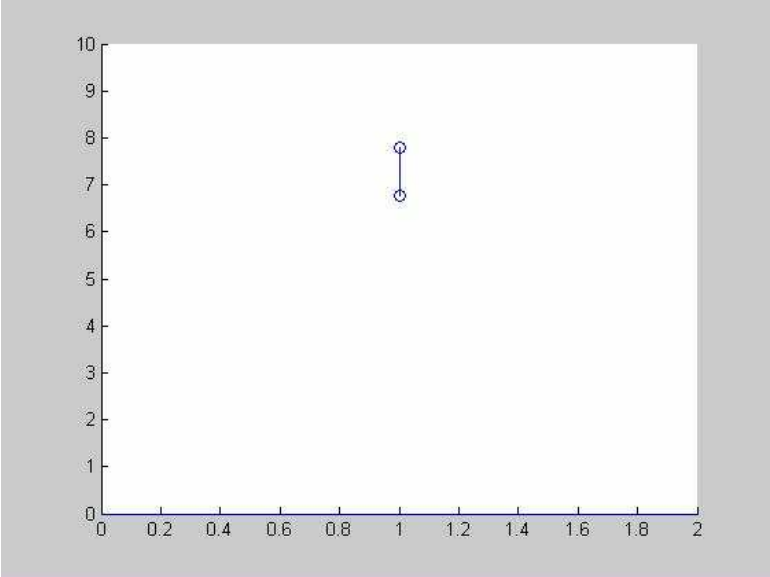

Figure 5.1. Single Spring.

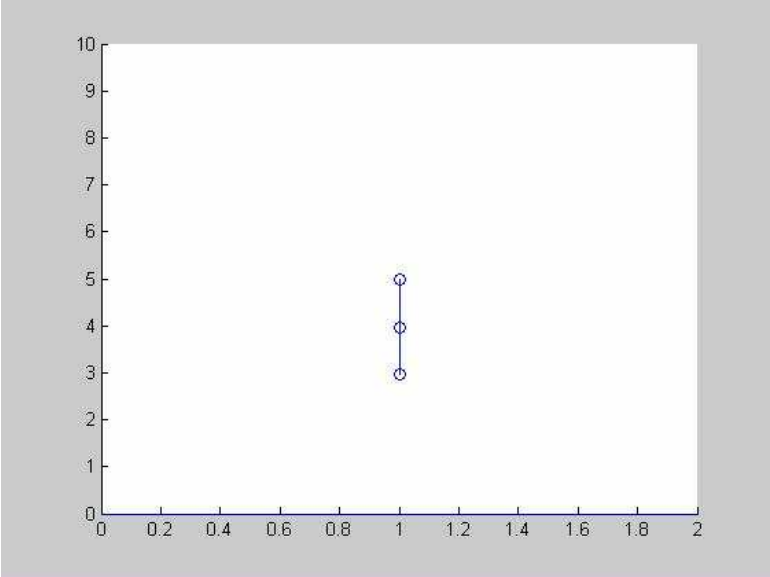

Figure 5.2. Double Spring.

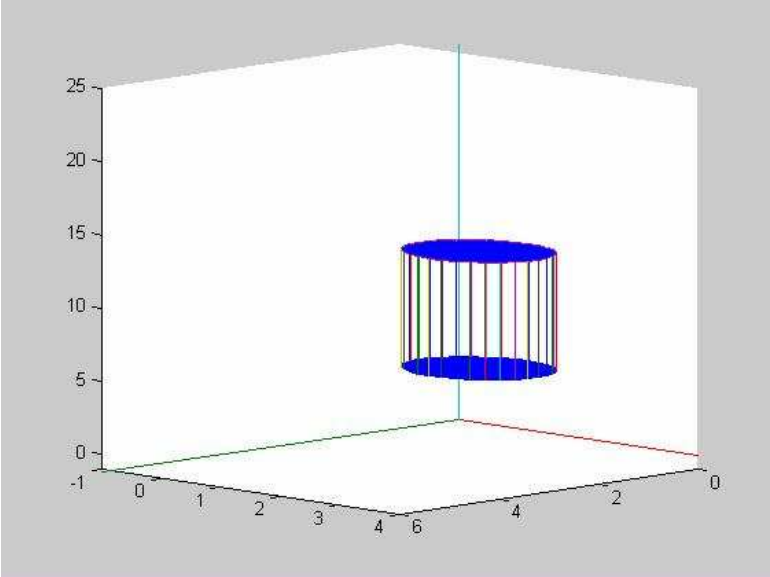

Figure 5.3. Cylinder.

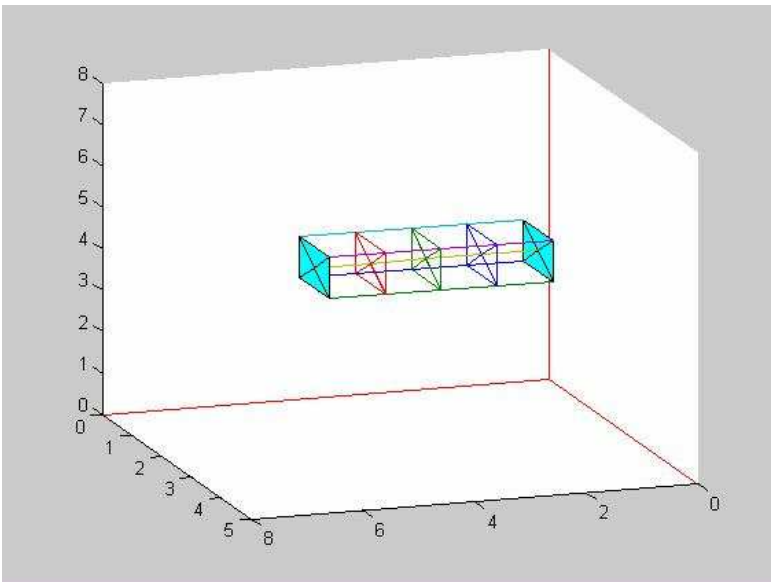

Figure 5.4. Truss.

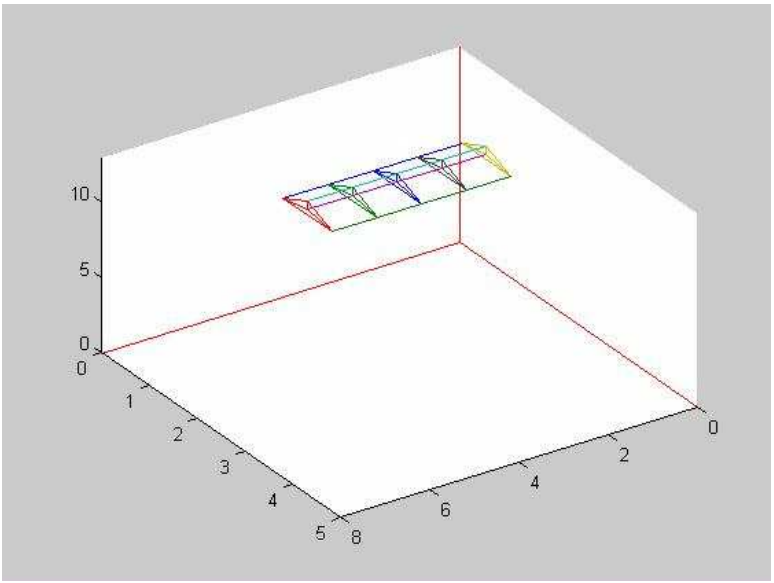

Figure 5.5. Prism.

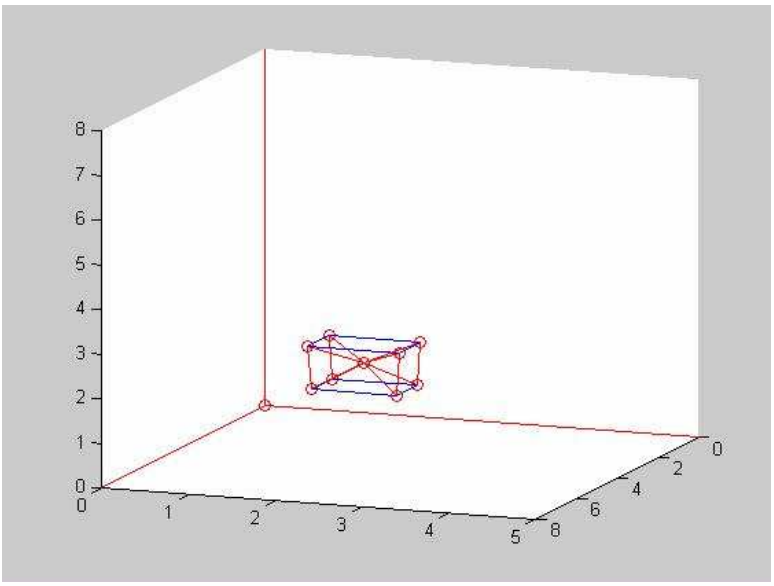

Figure 5.6. Cube.

5.3 Single Spring

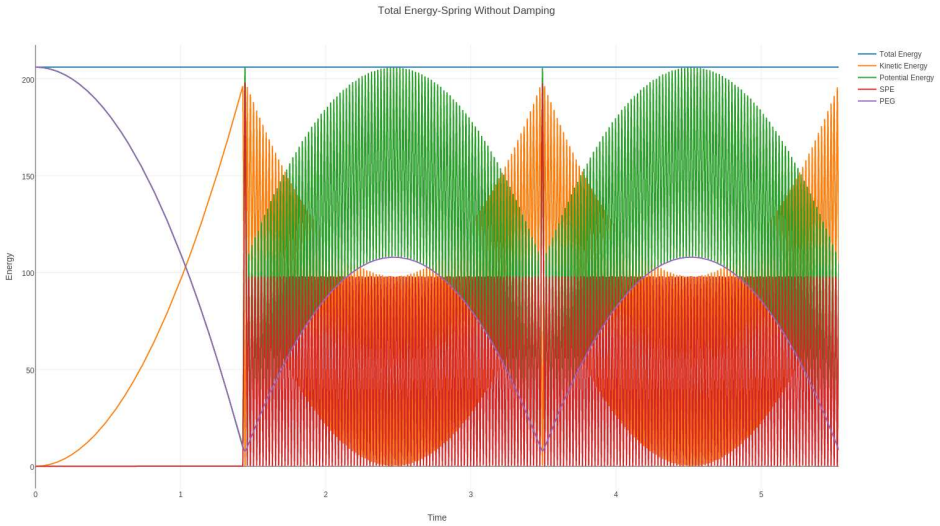

Figure 5.7. Energy Graph of Spring w/o Damping.

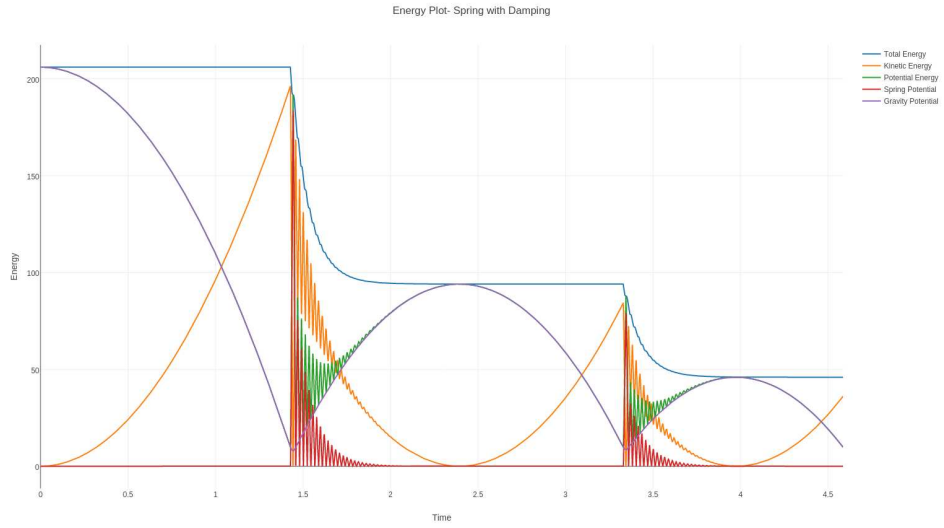

Figure 5.8. Energy Graph of Spring with Damping.

5.4 Double Spring

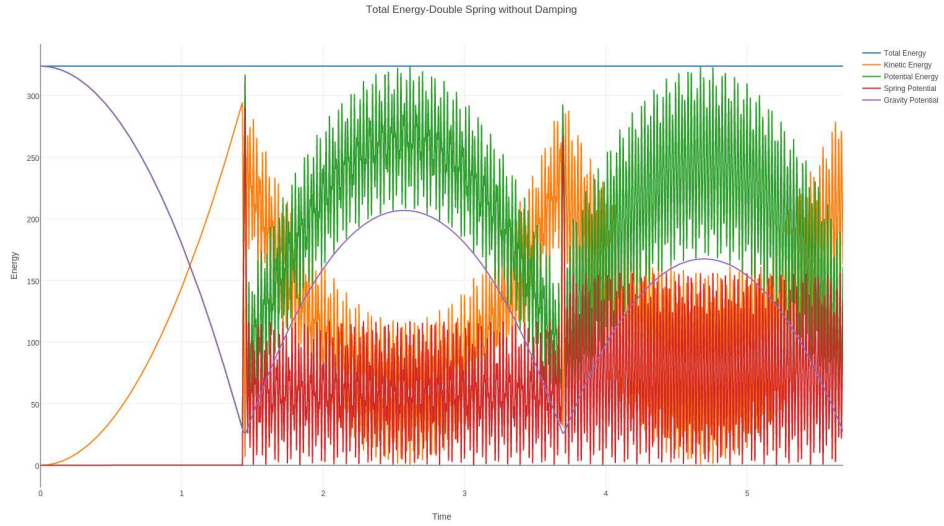

Figure 5.9. Energy Graph of Double Spring w/o Damping.

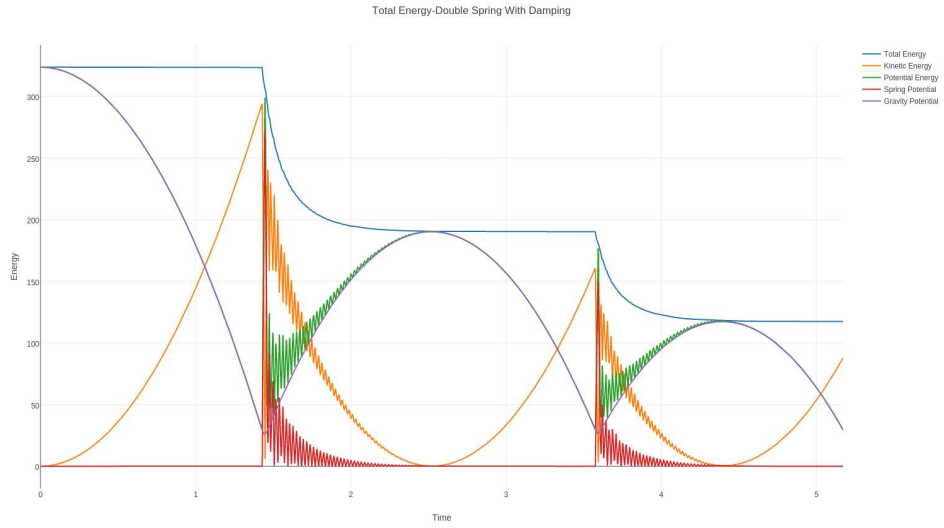

Figure 5.10. Energy Graph of Double Spring with Damping.

5.5 Cylinder

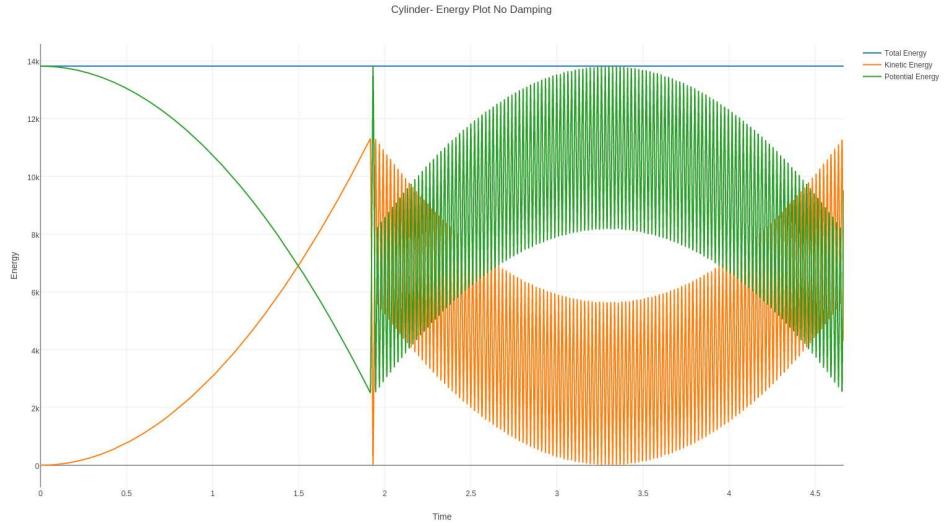

Figure 5.11. Energy Graph of Cylinder w/o Damping.

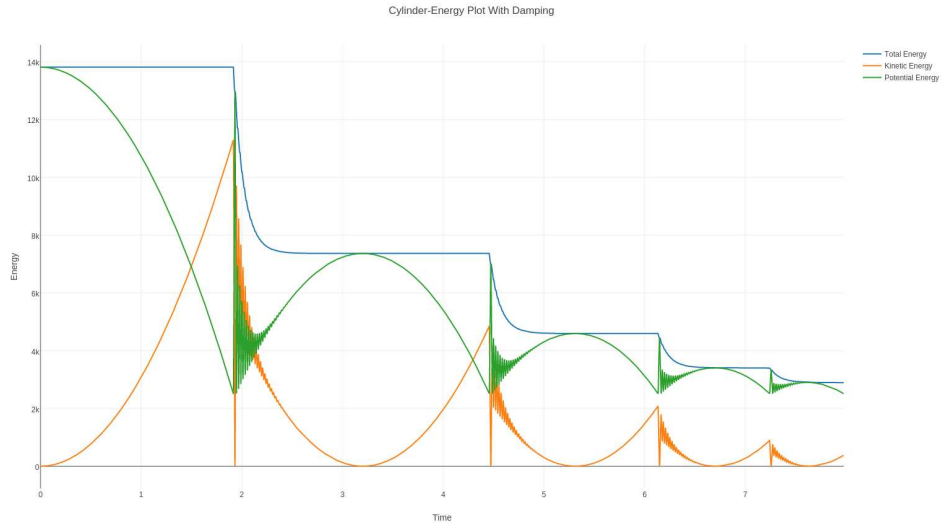

Figure 5.12. Energy Graph of Cylinder with Damping.

5.6 Truss

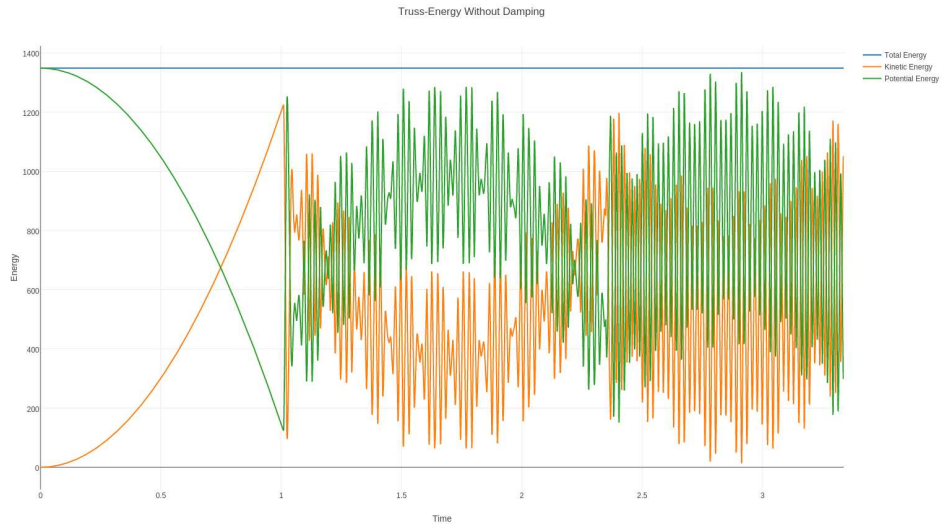

Figure 5.13. Energy Graph of Truss w/o Damping.

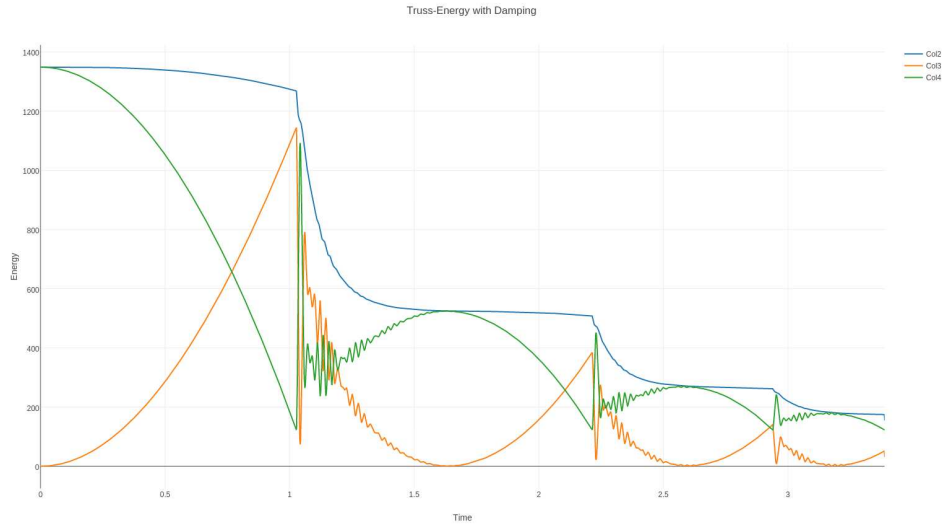

Figure 5.14. Energy Graph of Truss with Damping.

5.7 Prism

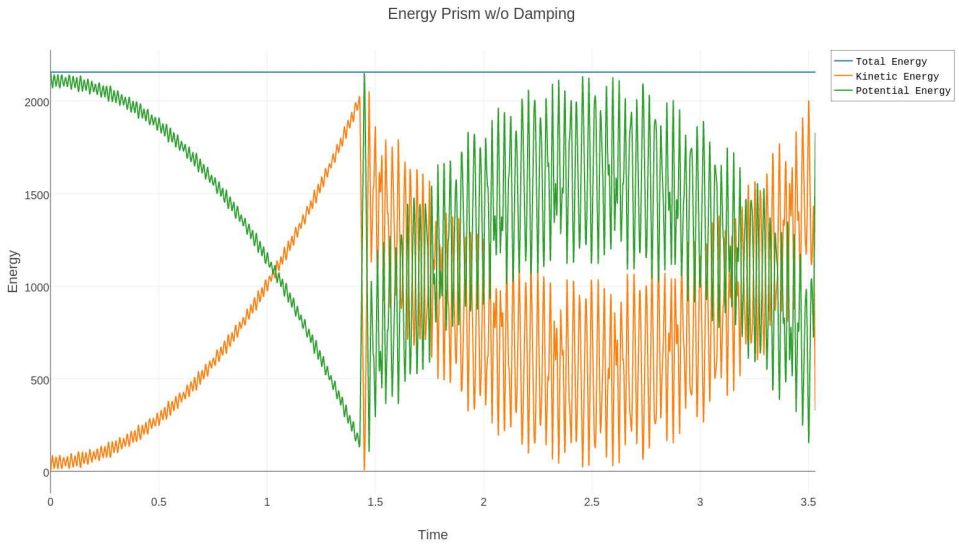

Figure 5.15. Energy Graph of Prism w/o Damping.

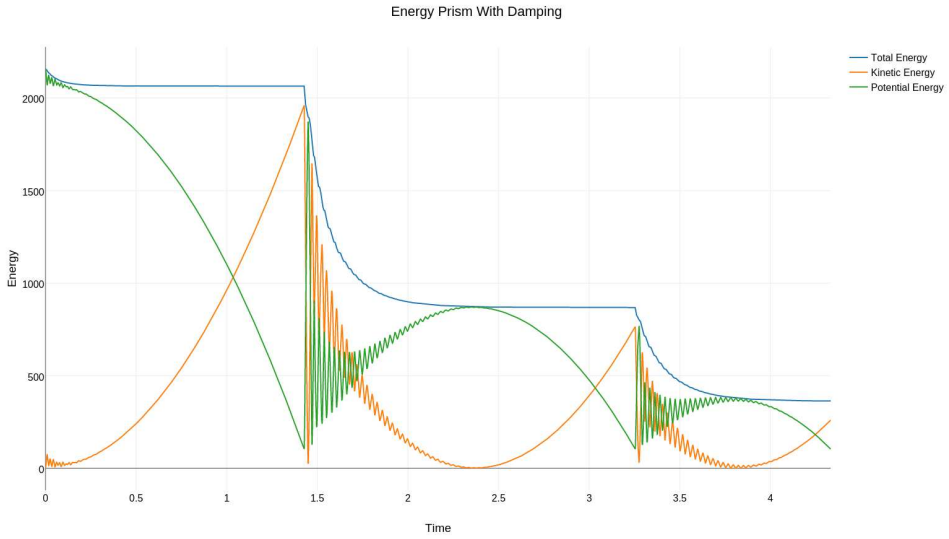

Figure 5.16. Energy Graph of Prism with Damping.

5.8 Cube

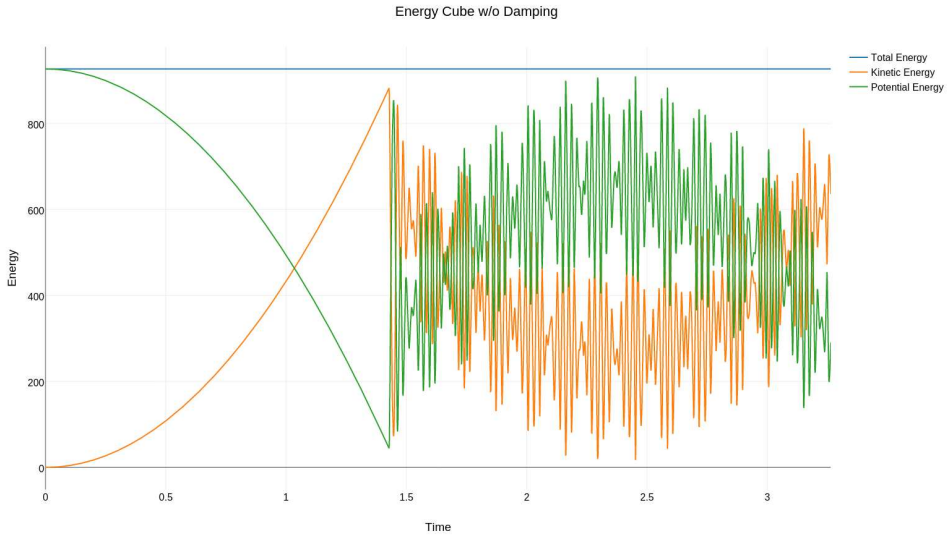

Figure 5.17. Energy Graph of Cube w/o Damping.

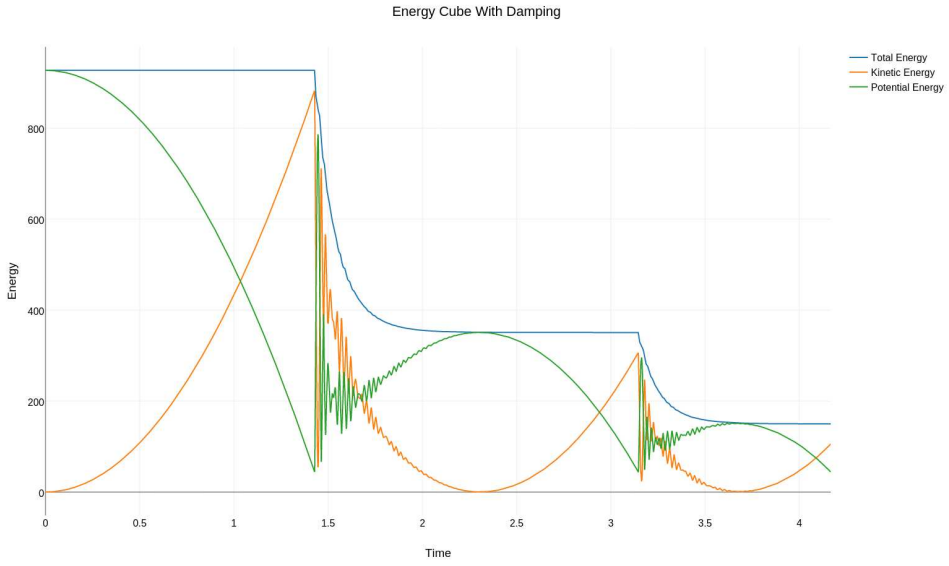

Figure 5.18. Energy Graph of Cube with Damping.

5.9 Complex Structure

The energy compensation for simpler objects is as above. For more complex structures we can divide the whole structure into small cubes. The cubes will have point masses on every corner and one at the center. We can compensate the energy of the colliding particles with the point mass at the center. The figure below shows an example of a cube with a point mass at center.

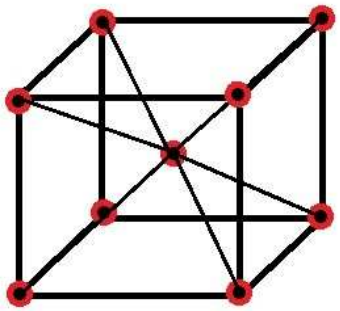

Figure 5.19. Cube Structure.

REFERENCES

[1] A. Chatterjee, "Three-dimensional indeterminate impacts in legged robotic locomotion," 2015.

[2] R. Sharma and B. Dash, "Carka samhita volume ii," *Chowkamba Sanskrit Series Office, Varanasi, India*, 1998.

[3] N. Al-Waili, K. Salom, and A. A. Al-Ghamdi, "Honey for wound healing, ulcers, and burns; data supporting its use in clinical practice," *The scientific world journal*, vol. 11, pp. 766–787, 2011.

[4] E. Park-Lee and C. Caffrey, "Pressure ulcers among nursing home residents: United states, 2004." *NCHS data brief*, no. 14, pp. 1–8, 2009.

[5] D. M. Smith, "Pressure ulcers in the nursing home," *Annals of internal medicine*, vol. 123, no. 6, pp. 433–438, 1995.

[6] I. Mohammad and H. Huang, "Shear sensing based on microstrip patch antenna," *Measurement Science and Technology*, vol. 23, p. 105705(5 pages), 2012.

[7] ——, "Pressure and shear sensing based on microstrip antennas," in *Proceedings of SPIE-Smart Structures and Materials and NDE for Health Monitoring and Diagnostics*, March 2012, san Diego, California, USA.

[8] ——, "Plantar pressure sensing using loop antenna sensors," in *Proceedings of the 5th ACM International Conference on Pervasive Technologies Related to Assistive Environments (PETRA)*, June 2012, heraklion, Crete, Greece.

[9] D. Bain, *Evaluation of Nightingale ProAxis Plus Bed with Regard to Dynamic Pressure Attributes*, Duncan Bain Consulting, Kings Langley, 2006, [Online; accessed 31-January-2013].

[10] M. Twiste and S. Rithalia, "Measurement System for the Evaluation of Alternating Pressure Redistribution Mattresses Using Pressure Relief Index and Tissue Perfusion- A Preliminary Study," *Wound Practice and Research*, vol. 16, no. 4, pp. 192–198, 2008.

[11] Z. Brush, A. Bowling, M. Tadros, and M. Russell, "Design and control of a smart bed for pressure ulcer prevention," in *Advanced Intelligent Mechatronics (AIM), 2013 IEEE/ASME International Conference on*. IEEE, 2013, pp. 1033–1038.

[12] D. Zhang and M. M. Yuen, "Cloth simulation using multilevel meshes," *Computers & Graphics*, vol. 25, no. 3, pp. 383–389, 2001.

[13] M. Matyka and M. Ollila, "Pressure model of soft body simulation," *Proceedings of Sigrad, UMEA*, pp. 29–34, 2003.

[14] R. A. Potyrailo, C. Surman, D. Monk, W. G. Morris, T. Wortley, M. Vincent, R. Diana, V. Pizzi, J. Carter, G. Gach, S. Klensmeden, and H. Ehring, "Rfid sensors as the common sensing platform for single-use biopharmaceutical manufacturing," *Measurement Science and Technology*, vol. 22, no. 8, 2011.

[15] Y.-H. Kim, K. Jang, Y. J. Yoon, and Y.-J. Kim, "A novel relative humidity sensor based on microwave resonators and a customized polymeric film," *Sensors and Actuators B: Chemical*, vol. 117, no. 2, pp. 315–322, 2006.

[16] I. Mohammad and H. Huang, "Pressure and shear sensing based on microstrip antennas," in *SPIE Smart Structures and Materials+ Nondestructive Evaluation and Health Monitoring*. International Society for Optics and Photonics, 2012, pp. 83 451D–83 451D.

[17] ——, "Monitoring fatigue crack growth and opening using antenna sensors," *Smart Materials and Structures*, vol. 19, no. 5, p. 055023, 2010.

[18] X. Xu and H. Huang, "Multiplexing passive wireless antenna sensors for multi-site crack detection and monitoring," *Smart Materials and Structures*, vol. 21, no. 1, 2012.

[19] A. Rodriguez and A. Bowling, "Solution to indeterminate multipoint impact with frictional contact using constraints," *Multibody System Dynamics*, vol. 28, no. 4, pp. 313–330, 2012.

[20] W. Stronge, *Impact Mechanics*. Cambridge University Press, 2000.

[21] Y.-B. Jia, M. Mason, and M. Erdmann, "Multiple impacts: A state transition diagram approach," *The International Journal of Robotics Research*, p. 0278364912461539, 2012.

BIOGRAPHICAL STATEMENT

Pranav Bharatbhai Parikh was born in Nadiad, Gujarat, India, in 1990. He is a proud son of Bharat Mahendrabhai Parikh, and Nayana Bharat Parikh (Nayana Dileep Munim, before marraige), and brother of proud sisters Rachana Bharat Parikh, and Vyoma Bharat Parikh. He graduated from St. Anne's High School, Nadiad in 2007. He received his Bachelor's Degree in Engineering (Mechatronics Engineering) from G. H. Patel College of Engineering and Technology-Sardar Patel University, Vallabh Vidhya Nagar, Gujarat, India in May 2011. He joined Larsen and Toubro, Industrial Automation department as Sr. Engineer, at Powai, Mumbai in August 2011. He left Larsen and Toubro in December 2013 and continued with his higher education from University of Texas at Arlington in January 2014. At University of Texas at Arlington he worked for the Robotics, Biomechanics, and Dynamics Systems Laboratory for Dr. Alan Bowling, while completing his thesis research.